



Gouthaman, S., Madhu, V., Kanemoto, S. O., Madurai, S. L., & Hamerton, I. (2019). Examining the Thermal Degradation Behaviour of a Series of Cyanate Ester Homopolymers. *Polymer International*, 68(10), 1666-1672. <https://doi.org/10.1002/pi.5886>

Peer reviewed version

Link to published version (if available):
[10.1002/pi.5886](https://doi.org/10.1002/pi.5886)

[Link to publication record in Explore Bristol Research](#)
PDF-document

This is the accepted author manuscript (AAM). The final published version (version of record) is available online via Wiley at <https://doi.org/10.1002/pi.5886> . Please refer to any applicable terms of use of the publisher.

University of Bristol - Explore Bristol Research

General rights

This document is made available in accordance with publisher policies. Please cite only the published version using the reference above. Full terms of use are available: <http://www.bristol.ac.uk/red/research-policy/pure/user-guides/ebr-terms/>

1 **Examining the Thermal Degradation Behaviour of a Series of** 2 **Cyanate Ester Homopolymers**

3 S. Gouthaman^a, M. Venkatesh^a, S.O. Kanemoto^{a,b}, M. Suguna Lakshmi^a, I. Hamerton^{c*}

4 ^a *Polymer Science & Technology Division, Central Leather Research Institute (CSIR – CLRI),*
5 *Chennai, 600 020, India.*

6 ^b *Macromolecular Research Team, Department of Inorganic Chemistry, University of Yaounde-*
7 *I, 812-Yaounde, Cameroon.*

8 ^c *Bristol Composites Institute (ACCIS), Department of Aerospace Engineering, School of Civil,*
9 *Aerospace, and Mechanical Engineering, Queen’s Building, University of Bristol, University*
10 *Walk, Bristol, BS8 1TR, U.K.*

11 **Abstract**

12 A series of thermally stable dicyanate monomers, containing different thermally stable structural
13 units, viz 2,2'-bis (4-cyanatophenyl)propane (DCDPP), bis-4-cyanato-biphenyl (DCBP), bis-4-
14 cyanato naphthalene (DCN), 3,3'-bis(4-cyanatophenyl) sulphide (DCTDP) and 3,3'-bis (4-
15 cyanatophenyl) sulphone (DCDPS), is prepared and the identity of the products confirmed by
16 FT-IR and NMR spectral methods. The corresponding cyanate homopolymers (designated by the
17 suffix HP) are prepared and their properties evaluated and compared. The composites were
18 analysed for their thermal stability and thermal degradation kinetics. The series of
19 homopolymers exhibit excellent thermal characteristics e.g. relatively high glass transition
20 temperatures of at least 215 °C, which were inversely proportional to the molecular weight
21 between the crosslinks, high thermal decomposition temperature, high integral procedural
22 decomposition temperature (IPDT), and high activation energies for the decomposition of the
23 cured resins. Determination of their limiting oxygen indices indicates that all the homopolymers
24 are characterized as 'self-extinguishing' materials.

25 **KEY WORDS:** *Cyanate esters, Homopolymers, Curing, Flame retardance, Thermogravimetric*
26 *analysis*

27 *Prof. I. Hamerton, e-mail: ian.hamerton@bristol.ac.uk, Tel.: +44 (0)117 3314799

28

29 **1. INTRODUCTION**

30 Cyanate ester resins have stimulated substantial interest, due to their exclusive combination of
31 properties, such as low water absorption, low dielectric constant and heat release rate, superior
32 strength, excellent bonding towards metals, glass and carbon matrices, low volatility while
33 curing, and high resistance towards high heat and high humid environments. Owing to their
34 excellent final cured properties, they find application as structural adhesives for making high
35 temperature resistant and light-weight advanced composites [1,2]. Cyanate esters have definite
36 advantages over bismaleimide (BMI) resins due to lower typical crosslink densities and higher
37 flexibility because of the high percentage of oxygen linkages present [3]. These attributes of
38 cyanate esters are reflected in the higher fracture toughness observed when incorporated into
39 epoxy resins in comparison with BMIs [4].

40 Cyanate ester resins are primarily used in the field of aerospace materials, in dielectric
41 components, printed circuit boards, coatings and other applications requiring high temperature
42 resistant and moisture resistant materials. These applications are the consequence of their high
43 mechanical strength, high moisture resistance, low dielectric loss, low volatility during the cure,
44 and low toxicity [5-6]. In recent years, many new cyanate monomers have emerged especially
45 the dicyanates containing aromatic ether [7], ketone [8,9], 2,7-dihydroxynaphthalene [10],
46 polyurethane [11], thiophenols [12,13], silicones [14,15] and phosphorus [16,17]. Though
47 cyanate esters are known to exhibit excellent thermal properties, investigations into the thermal
48 behaviour, thermal stability and thermal degradation kinetics studies using different
49 mathematical models under non-isothermal and isothermal conditions are more limited beyond
50 very basic cyanate esters [18,19]. The trend for increased use of cyanate esters is due to the

51 growing demand for light-weight, low dielectric loss, high heat resistant structures for
52 manufacturing military aircraft [4,20-27]. Consequently, in this study, a detailed and systematic
53 evaluation is analyzed and discussed, especially concerning the thermal properties of the
54 homopolymers.

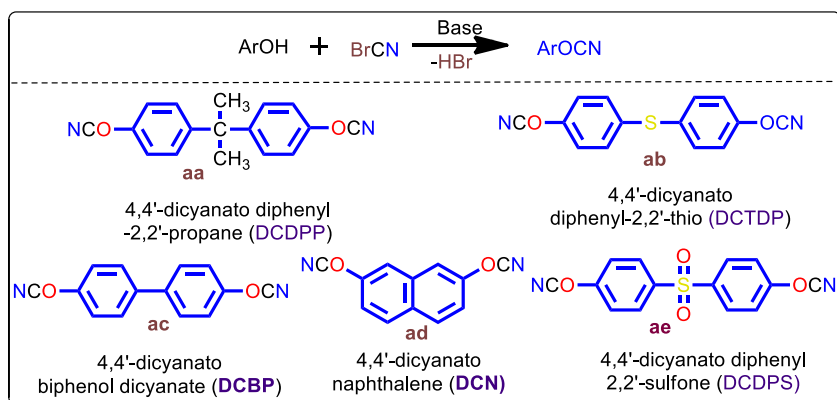
55 2. MATERIALS AND METHODS

56 2.1. Materials

57 2,2-Bis(4-hydroxyphenyl)propane (99%), 1,4-naphthalene diol (99%), 4,4'-biphenyldiol (97%),
58 4,4'-thiodiphenol (99%), 4,4'-sulphonyl diphenol (98%), and cyanogen bromide (99%) were
59 purchased from Aldrich Chemical Company. Triethylamine, acetone and methanol (Analytical
60 Reagent grade) were purchased from S.D. Fine Chemicals Pvt. Ltd., Mumbai, India.

61 2.2. Synthesis of 2,2'-bis(4-cyanatophenyl)propane (DCDPP)

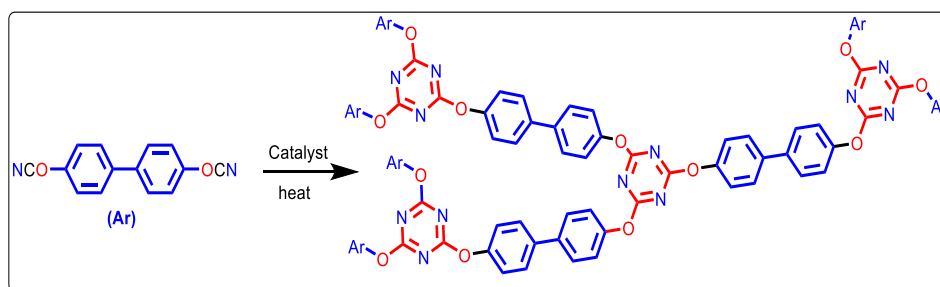
62 A batch scale of cyanate ester (100g) was synthesized at 0 °C by the reaction of cyanogen
63 bromide (74.6 g, 0.7 mol.) and bisphenol A (81 g, 0.35 mol.). Triethylamine (90 g, 0.89 mol.)
64 was added to catalyse the reaction and to absorb the evolved HBr to yield salts of tri-
65 ethylamine hydrobromide (Fig. 1 and Fig. S1). The synthesis was carried out in a three-necked
66 round-bottomed flask equipped with a mechanical stirrer and a nitrogen inlet was charged a
67 cooled solution of bisphenol A and cyanogen bromide in acetone. Triethylamine was added
68 dropwise under continuous stirring in an ice bath and, after complete addition, the reaction
69 mixture was stirred for a further period of one hour while maintaining the ice bath temperature at
70 0 °C and filtered under vacuum. The reaction mixture was filtered and, the filtrate was poured
71 into a large amount of cold distilled water (1L) to precipitate the bisphenol A cyanate ester,
72 DCDPP, Fig 1(a), from the solution. The crude product was further purified by recrystallization
73 in methanol: water (1:1 V/V). The product was a white crystalline with 76 g yield (80%) and
74 m.p. 75-78 °C.



75

76 Fig. 1. Reaction scheme for the preparation of the dicyanate monomers (a-e).

77 The remaining cyanates: DCTDP (RMM 268; m.p. 79 °C solid, white colour), Fig 1(b),
 78 DCBP (RMM 236; m.p. 82 °C solid, brown colour), Fig 1(c), DCN (RMM 210; m.p. 80 °C,
 79 solid, dark brown colour), Fig 1(d), and DCDPS (RMM 300; m.p. 81 °C, solid, light brown
 80 colour), Fig 1(e) were prepared from their respective dihydroxy compounds by employing the
 81 same procedure [19,20]. All the products were characterized by FT-IR and ¹³C NMR
 82 spectroscopic techniques. Each cyanate ester (100 parts) was homopolymerized (Fig. 2) by
 83 heating at 140 °C for 3 h, 160 °C for 2 h and followed by a post-curing at 180°C for 4h and 200
 84 °C for 2 h.



85

86

Fig. 2. General reaction scheme for the cyclotrimerisation of the dicyanate monomers.

87 2.3. Characterisation

88 Fourier Transform Infrared (FT-IR) spectra were obtained using a Nicolet model 20DXB
89 spectrophotometer with KBr pellets for solid specimens within scanning range of 400-4000 cm^{-1}
90 at the resolution of $< 0.1 \text{ cm}^{-1}$. A JOEL ECA-500 nuclear magnetic resonance (NMR)
91 spectrometer was used to carry out the analyses at 298K using TMS standard and CDCl_3 solvent.
92 ^1H NMR spectra were recorded at 500 MHz and ^{13}C NMR at 125 MHz. The thermal stabilities of
93 the cured polymers were determined using TGA Q50-TA thermal analyzer. The
94 thermogravimetric analysis (TGA) curves were recorded between 30-800 $^\circ\text{C}$ for cured HP
95 samples (10-15 mg) at a heating rate of $10^\circ\text{C}/\text{min}$ and under a flowing nitrogen atmosphere (10
96 cm^3/min). The differential scanning calorimetric (DSC) studies were conducted on DSC Q200
97 TA instrument at the heating rate of $5^\circ\text{C}/\text{min}$ between 0-300 $^\circ\text{C}$. Nitrogen gas flow rate was kept
98 at the rate of $10 \text{ cm}^3/\text{min}$. Scanning electron microscopic (SEM) analysis was performed using a
99 JEOL 400 microscope on the fractured surface of the cured neat resin applying an accelerating
100 voltage of 5kV; the fractured samples were first sputtered with carbon.

101 3. RESULTS AND DISCUSSIONS

102 3.1. Characterization of monomers by FT-IR and ^{13}C NMR spectroscopy

103 FT-IR spectra of the dicyanate monomers (see Supplementary data, Fig. S2) display the
104 characteristic (O-C \equiv N) doublet around 2200 cm^{-1} , confirming the presence of the cyanate group,
105 while the ^{13}C NMR spectra (Fig. S3) showed the resonances corresponding to the cyanate
106 functional groups and all the carbons present in the compounds. The characteristic signals of the
107 OCN carbons attached to the aromatic rings for DCDPP, DCBP, DCN, DCTDP, and DCDPS
108 were observed at 116, 109.4, 116.9, 106.5, and 111.6 ppm respectively. The aromatic carbons
109 appeared in the range 129-188 ppm for DCBP, 118-153 ppm for DCDPP, 118-162 ppm for
110 DCDPS, 106-154 ppm for DCN, and 116-156 ppm for DCTDP respectively.

111 3.2. DSC analysis

112 3.2.1. Thermal behaviour

113 From the DSC curves (Fig. S4) of the cured samples of cyanate homopolymers systems,
114 DCDPP-HP, DCBP-HP, DCN-HP, DCTDP-HP, and DCDPS-HP exhibited their glass transition
115 temperatures (T_g) at 247, 215, 256, 253, and 215 °C respectively. The high T_g of the
116 homopolymer systems (> 200 °C) is due to the presence of the triazine rings, formed by the
117 cyanate monomers. Amongst the homopolymer systems, DCN-HP exhibits the highest T_g : the
118 naphthalene moiety has a rigid, planar structure, which packs more readily through π - π stacking
119 [21-22]. The mass loss occurred up to 130 °C is because of the elimination of solvent and
120 moisture for purification of polymers. Thermal stability of DCDPP-HP shows the highest and
121 DCN-HP shows lowest due to the fused naphthalene core. Mainly, DCDPP-HP and DCPPS-HP
122 show higher resistance to heat because of the presence of sulfone and dimethyl propane groups
123 and which contribute to the single degradation step. On the other hand, the remaining three
124 homopolymers display two degradation steps: the first due to the single bond scissions and the
125 second could be the pyrolysis of the cyanurate rings (380 °C- 420 °C). The mass loss occurred up
126 to 130 °C is because of the elimination of solvent and moisture for purification of polymers.
127 Thermal stability of DCDPP-HP shows the highest and DCN-HP shows lowest due to the fused
128 naphthalene core.

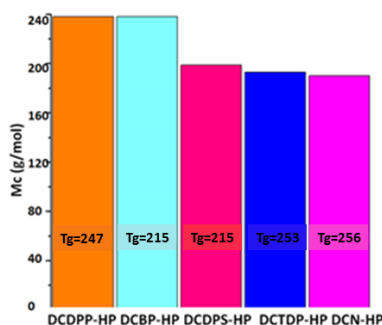
129 3.2.2. Estimation of M_c

130 The estimation of the molecular weights between adjacent crosslinks (M_c) helps to understand
131 the development of the physical network structure of the polymer since M_c is inversely
132 proportional to the crosslink density. The latter is one of the vital structural parameters that aid
133 knowledge of the influence of changes in the segmental motions, which are reflected in the
134 mechanical properties of thermoset polymers. When the number of crosslink junctions increases,

135 the crosslink density increases and this to a concomitant increase in T_g . Hence, the relationship
 136 between T_g and M_c can also be correlated with the crosslink density of the polymer. The M_c
 137 values for the homopolymer systems presented in this article were estimated using an empirical
 138 equation 1 [23].

$$139 \quad M_c = \frac{3.9 \times 10^4}{T_g - T_g^0} \quad (1)$$

140 T_g^0 is the glass transition temperature of the non-crosslinked polymer.



141

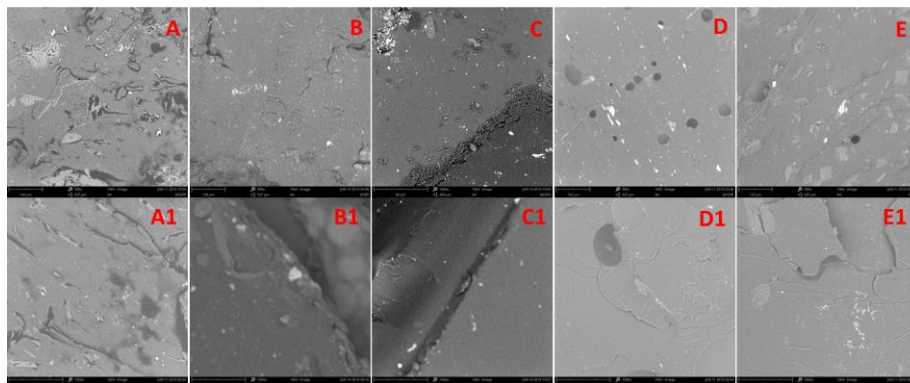
142 Fig. 3. Correlation study presenting molecular weight between the crosslinks (M_c) for the
 143 different cyanate ester homopolymers

144 Cyanate ester homopolymers show a range of M_c values from 198 g.mol^{-1} to 240 g.mol^{-1} (Fig.
 145 3). DCN-HP has the lowest M_c value (198 g.mol^{-1}) following by DCTDP-HP, then DCDPS-HP,
 146 DCBP-HP, and DCDPP-HP (240 g.mol^{-1}). Those values depend on the planar structure of the
 147 aromatic ring and the ability of localized motions of chain segments [24]. In this reason, amongst
 148 the homopolymer systems, DCN-HP exhibits the lowest M_c value.

149 3.3. Fracture analysis

150 The cured homopolymers were subjected to SEM analysis to analyse the fractured surfaces. In
 151 general, the surfaces (Fig. 4) show similar, complex morphologies that are typical of shear

152 failure; all the polymers show elastic deformation zones that predominate. Previously, a
153 commercial cyanate ester (AroCy B-30), which shares an identical chemical structure to DCDPP,
154 was analysed using similar conditions.[25]



155
156 Fig. 4. Scanning electron microscopic images of the cured cyanate homopolymers with 500X
157 (A-E) and 1000X (A1-E1) for DCDPP (A & A1), DCBP (B&B1), DCDPS (C&C1), DCTDP
158 (D&D1), and DCN (E&E1)

159

160 3.4. Thermogravimetric analysis

161 3.4.1. Thermal properties

162 The thermal stabilities of the cured homopolymers were examined using the TGA technique: the
163 thermal stability of polymers was evaluated by a number of parameters (Table 1) may lead to
164 contradictory results, in terms of the onset temperature for degradation (DCDPP-HP), lowest rate
165 of mass loss (DCN-HP), or highest char yield (DCN-HP and DCTDP-HP). The maximum
166 decomposition temperature (MDT) is the temperature at which the highest rate of thermal
167 degradation is recorded.

168

169

170

171 Table 1. Thermal properties of cyanate homopolymer

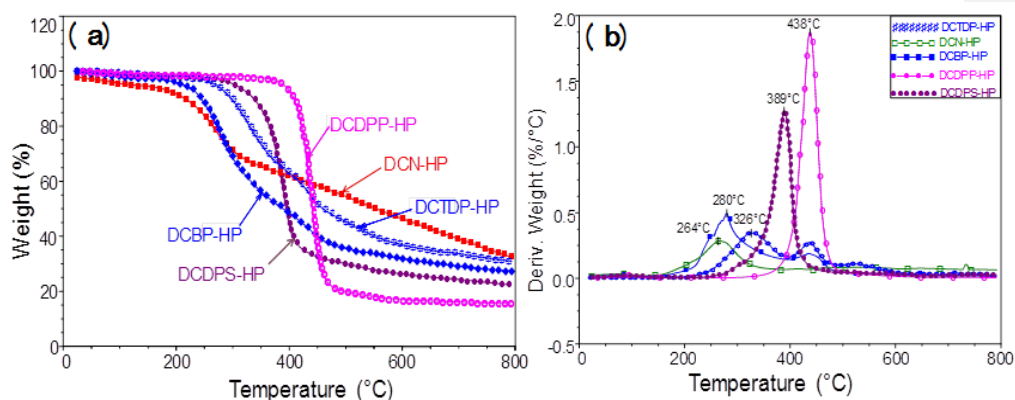
Polymer	Initial decomposition temperature IDT (°C)	Mass loss (%)			Maximum decomposition temperature MDT (°C)	Char residue at 800°C CR (%)
		3	15	30		
DCBP-HP	246	219	273	288	327	28
DCN-HP	229	196	260	274	264	35
DCTDP-HP	250	319	346	441	327	31
DCDPP-HP	388	411	434	446	438	16
DCDPS-HP	323	350	365	377	389	22

172

173 These data were not acquired using hyphenated apparatus in which chemical speciation was
 174 possible. Consequently, inferences are drawn based on the profile of the thermal degradation and
 175 comparisons of masses lost, with chemical moieties found within the polymer backbones. The
 176 TGA data for the homopolymers (Fig. 5a) suggests that, beyond the differences in onset
 177 temperatures, there are similarities in the degradation mechanism observed for DCBP-HP and
 178 DCTDP-HP. DCDPS-HP and DCDPP-HP both similarly lose mass in a single drop. The mass
 179 loss observed up to 150 °C is probably due to the removal of water, which is used for
 180 recrystallization along with methanol.

181 DCN-HP shows the maximum decomposition temperatures all exceed 260 °C, and this occurs
 182 around 400 °C for the best performing systems (Fig. 5b), which contain sulphur in the backbone
 183 structure.

184



185

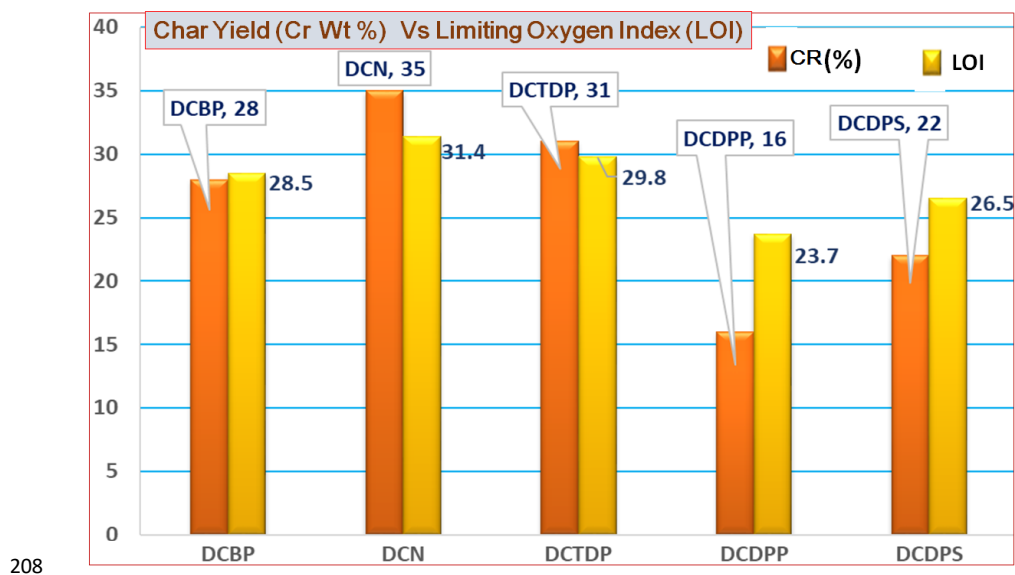
186 Fig. 5. TGA data (a) and DTG data (b) for the homopolymer systems carried out under N₂
 187 atmosphere at a heating rate of 10°C/min.

188 The thermal decomposition of aromatic polycyanurates goes through a common mechanism
 189 which begins with thermolytic cleavage of the resin backbone and culminates with decyclization
 190 of the cyanurate rings around 300 °C, followed by char formation; these data are in good
 191 agreement with previous reports [26-28]. However, the other onsets can be attributed to two
 192 different species already present in the treated sample and not only formed during TGA
 193 execution, which showed the first onset around 450 °C corresponding to the decomposition into
 194 gaseous sulfonyl-di-benzene or propane-2,2-diyldibenzene unit. The char yields observed are
 195 typical for di-functional aromatic dicyanate homopolymers and DCN-HP, with the highest
 196 aromatic content, predictably shows the highest char yield (Table 1); DCDPP-HP with the
 197 greatest aliphatic character, the lowest. The flame-retardant property was found out from the
 198 limiting oxygen index (LOI) value, using the empirical formulae proposed by Van Krevelen *et*
 199 *al.* [29]. A numerical index, the LOI represents the minimum concentration of oxygen required
 200 to support the combustion of a polymer in the particular air mixture. Thus, higher LOI values
 201 represent better flame retardancy.

202
$$LOI = 17.5 + 0.4CR \quad (2)$$

203 where, *LOI* = limiting oxygen index, and *CR* = yield of char residue at 800°C.

204
 205 The homopolymer systems show the highest LOI values, which fall between 23-30, where values
 206 of $LOI < 20.95$, $LOI < 28.0$, and $LOI < 100$ are considered to represent 'flammable', 'slow-
 207 burning', and 'intrinsically non-flammable' materials respectively (Fig. 6).



209 Fig. 6. The comparison of char yield vs. LOI to the cyanate system, the labelled (orange is CR
 210 (%), Yellow is LOI (%))

211
 212 Using a more detailed description, the polymers possessing $LOI \geq 20.95$ and ≥ 26.0 are
 213 considered as 'marginally stable' and 'self-extinguishable' materials, respectively [30-32].

214 According to these criteria, all the homopolymer systems (except DCDPP) have exhibited 'self-
 215 extinguishing' characteristics.

216

217 **3.4.2. Determination of activation energy**

218 Thermogravimetric analysis was used for the determination of the kinetics of the thermal
 219 degradation of the polymers. The thermal degradation of the cured system was carried out at a
 220 heating rate of 10K min^{-1} under a flowing nitrogen atmosphere. The activation energy and order
 221 of reaction (n) were predicted by using the integral methods of the Broido, Horowitz-Metzger,
 222 and the Coats-Redfern models [334-35] derived from the Arrhenius equation.

223 The basic equation used to describe decomposition reactions is

$$224 \quad \frac{dy}{dt} = k(T)f(y) \quad (34)$$

225 where the rate constant $k(T)$ and $f(y)$ were functions of temperature, and conversion respectively
 226 was defined as

$$227 \quad y = \frac{M_0 - M_t}{M_0 - M_f} \quad (45)$$

228 where M_0 : initial sample weight, M_t and M_f were the weight at time t and final sample weight,
 229 respectively. Usually, k is assumed to follow the Arrhenius relationship:

$$230 \quad k = A \exp\left(\frac{-E}{RT}\right) \quad (65)$$

231 The reaction rate may be written as follows.

$$232 \quad \frac{dy}{dt} = \frac{dy}{dT} \frac{dT}{dt} = \beta \frac{dy}{dT} \quad (76)$$

233 Thus, change in mass vs. temperature can be written as

$$234 \quad \frac{dy}{dT} = \frac{A}{\beta} \exp\left(\frac{-E_a}{RT}\right) f(y) \quad (87)$$

235 The Coats-Redfern equation is as follows:

236 The integral form of Eq. 8 from initial temperature, T_i corresponding to a degree of conversion

237 m_0 , to a peak temperature, T_{\max} , can be written as

$$238 \quad \int_0^y \frac{dy}{f(y)} = \frac{A}{\beta} \int_{T_0}^{T_r} \exp\left(-\frac{E_a}{RT}\right) dT \quad (98)$$

239 Using an approximation, Broido rearranged Eq (87).

$$240 \quad \ln\left[\ln\frac{1}{y}\right] = -\frac{E_a}{R} \frac{1}{T} + \left(\frac{R}{E_a} \frac{A}{\beta} T_{\max}^2\right)_a \quad (109)$$

$$241 \quad \ln\left[\frac{-\ln(1-y)}{T^2}\right] = \ln\frac{AR}{\beta E_a} \left(1 - \frac{2RT}{E_a}\right) - \frac{E_a}{RT} \quad \text{for } n = 1 \quad (110)$$

242 and the modified equation of Horowitz-Metzger is given by:

$$243 \quad \ln(1-y) = \frac{E_a(T-T_p)}{R(T_p)} \quad \text{for } n = 1 \quad (121)$$

244 All of the models used give approximations since the decomposition of the systems involves

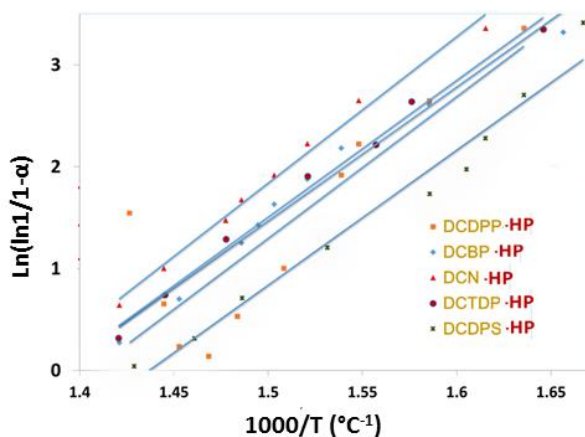
245 several, often coincident or sequential reactions [26-28]. The Horowitz-Metzger model assumes

246 a first-order reaction and uses the simplified exponential integrals to obtain the above equation.

247 The Broido model considers the thermal decomposition process to be a first-order reaction. The

248 Coats-Redfern model, when $n = 1$, was considered here for the activation energy calculations

249 [36]. The parameters used were: T is the absolute temperature, α is the conversion at temperature
 250 T , y is the fraction of initial molecules and not yet decomposed, T_{\max} the absolute temperature of
 251 maximum reaction rate, β is the rate of heating, A is the frequency factor, DT_{\max} is the maximum
 252 decomposition temperature, $\theta = T - DT_{\max}$, R is the gas constant and E_a is the activation energy. A
 253 plot of $\ln(\ln 1/y)$ in case of Broido's method, $\ln[-(1-y)/T^2]$ in case of Coats-Redfern method,
 254 and $(1-y)$ in the case of the Horowitz-Metzger method; vs. $1000/T$ for major degradation events
 255 yielded plots with linear portions. The changes in gradients are consistent with the different steps
 256 in the thermal degradation mechanism [26]. The cured samples of homopolymer systems were
 257 subjected to the kinetic analysis and are shown in Fig. 7, for the Horowitz-Metzger model.



258
 259 Fig. 7. The plots for the calculation of activation energies for homopolymers using the Horowitz-
 260 Metzger model

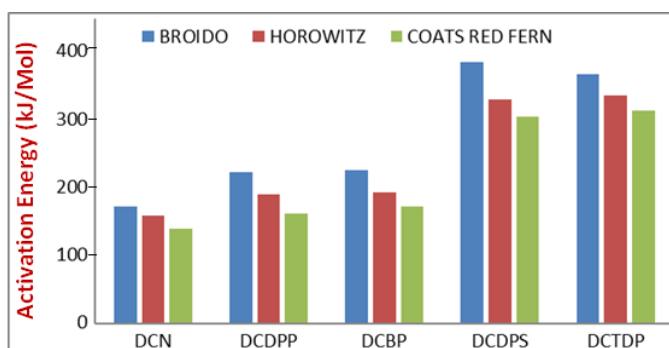
261 The kinetic parameters and the correlation coefficient (R^2) values of each system are summarized
 262 in Table 2.

263 Table 2 Comparison of kinetic parameters for the thermal degradation of the homopolymers using
 264 different models.

Polymer	Models					
	Broido		Horowitz-Metzger		Coats-Redfern	
	E_a (kJ.mol ⁻¹)	R^2	E_a (kJ.mol ⁻¹)	R^2	E_a (kJ.mol ⁻¹)	R^2
DCBP-HP	225	0.952	193	0.935	173	0.919
DCN-HP	173	0.970	159	0.964	140	0.953
DCTDP-HP	367	0.959	336	0.950	314	0.943
DCDPP-HP	223	0.933	190	0.899	163	0.866
DCDPS-HP	385	0.995	329	0.993	305	0.991

265 E_a = activation energy (kJ.mol⁻¹); R^2 = correlation coefficient.

266 While there are some differences in the activation energies (E_a) calculated, the trends observed
 267 are consistent between the different models and the E_a values were generally found to be in the
 268 following order for the models applied: Broido>Horowitz-Metzger>Coats-Redfern (Fig. 8). In
 269 the homopolymers, the E_a values derived using the Broido model fell between 173 - 385kJ/mol.



270
 271 Fig. 8. Comparison of activation energies for the thermal degradation of the homopolymers using
 272 different models.

273
 274 These values obtained for all the neat resins are higher than values that have previously been
 275 reported for the bisphenol E cyanate ester based on bisphenol E, 2,2'-bis(4-
 276 cyanatophenyl)ethylidene, (67 kJ mol⁻¹) [37] and a cyanate ester functional benzoxazine (100 kJ

277 mol⁻¹) [38] respectively. Within the data set, the highest activation energies calculated for the
278 thermal degradation of the homopolymers were obtained for the sulphur-containing
279 functionalized cyanate monomers (DCTP and DCDPS). The presence of sulphur plays a vital
280 role and the evolution of nonflammable gases (*e.g.* oxides of sulphur) during the degradation
281 may condense on the remaining polymer, thus diluting oxygen concentration at the polymer
282 surface, starving the flame, and serving as a free-radical flame front scavenger to inhibit
283 degradation of the polymers [39].

284

285

286 Five polycyanurate homopolymers displaying similar degrees of crosslink density, but
287 differing in terms of their molecular rigidity, were analysed for their thermal degradation
288 behavior, flame retardancy, and fracture properties. The homopolymers are all based on aromatic
289 monomers and so the high carbon content in the structure of homopolymers and presence of
290 nitrogen yields moderately high char yields (ranging from 16-35%, with DCDPP, containing an
291 aliphatic bridge, having the lowest value, and DCN, with no aliphatic character, the highest). The
292 activation energies (determined using the Broido model) for the decomposition behaviour of the
293 homopolymers revealed a wide variation, from 173 kJ/mol for DCN to 385 kJ/mol for DCDPS,
294 with the highest values in the data set being observed for homopolymers derived from simple
295 monomers.

296 **Acknowledgement:** One of the authors (MSL) would like to thank Dr. BSR Reddy, Retired
297 Emeritus Scientist, for his help and support. The author MSL also thank The CSIR-CLRI for the
298 financial support provided under MMP-06/18.

299

Formatted: Font color: Auto

300 **REFERENCES**

- 301 [1] Hamerton I., Hay J.N. *High Perform. Polym.*, 1998; 10(2): 163-174.
- 302 [2] Zhang Z., Liang G., Wang X., Adhikari S., Pei J., *High Perform. Polym.* 2013; 25: 427-435
- 303 [3] Fang T., Shimp D.A., *Prog. Polym. Sci.*, 1995; 20(1): 61-118
- 304 [4] Abed J.C., Mercier R., McGrath, J.E., *J. Polym. Sci. A Polym. Chem.* 1997; 35(6): 977-987
- 305 [5] Hamerton I. *Chemistry and Technology of Cyanate Ester Resins*. Glasgow: Blackie
- 306 Academic; 1994
- 307 [6] Tao Q., Gan W., Yu Y., Wang M., Tang X., Li S. *Polymer*, 2004; 45(10): 3505-3510
- 308 [7] Anuradha G., Sarojadevi M., *J. Polym. Res.*, 2008; 15(6): 507-514
- 309 [8] Fernandez A.M., Posadas P., Rodriguez A., Gonzalez L., *J Polym. Sci. A Polym. Chem.*,
- 310 1999; 37(16): 3155-3168
- 311 [9] Laskoski M., Dominguez D.D., Keller T.M., *J. Polym. Sci. A Polym. Chem.*, 2006; 44(15):
- 312 4559-4565
- 313 [10] Yan H.Q., Chen S., Qi G.R., *Polymer*, 2003; 44(26): 7861-7867
- 314 [11] Pazhanikumar T., Sivasankar B., Sugumaran T., *High Perform. Polym.*, 2007; 19(1): 97-112
- 315 [12] Bauer M., Bauer J., *J. Appl. Polym. Sci.*, 2008; 110(1): 8-17
- 316 [13] Lin R.H., Hong J.L., Su A.C., *Polymer*, 1995; 36(17): 3349-3354
- 317 [14] Maya E.M., Snow A.W., Buckley L.J., *Macromolecules*, 2002; 35(2): 460-466
- 318 [15] Guenther A.J., Yandek G.R., Wright M.E., Petteys B.J., Quintana R., Connor D.,
- 319 *Macromolecules*, 2006; 39(18): 6046-6053
- 320 [16] Lin C.H., Yang K.Z., Leu T.S., Lin, C.H., Sie, J.W., *J. Polym. Sci. A Polym. Chem.*, 2006;
- 321 44(11): 3487-3502
- 322 [17] Abed J.C., Mercier R., McGrath J.E., *J. Polym. Sci. A Polym. Chem.*, 1996; 35(6): 977-987
- 323 [18] Hamerton I, Emsley A.M., Howlin B.J., Klewpatinond P., Takeda S., *Polymer*, 2004; 45(7):
- 324 2193-2199
- 325 [19] Pankratov V.A., Vinogradova S.V., Korshak V.V., *Russ. Chem. Rev.*, 1977; 46(3): 278
- 326 [20] Lee J.Y., Jang J., *J. Polym. Sci. A Polym. Chem.*, 1999; 37(4): 419-425
- 327 [21] Wang C.S., Lee M.C., *Polymer*, 2000; 41(10): 3631-3638
- 328 [22] Bauer R.S., *ACS Symp. Ser. Am. Chem. Soc.*, Washington, DC, 1979; 114
- 329 [23] Zhavoronok E.S., Senchikhin I.N., Roldugin V.I., *Polym. Sci. Ser. A*, 2011; 53(6): 449.
- 330 [24] Lesser, A.J., Crawford, E., *J. Appl. Polym. Sci.*, 1997; 66(2): 387-395.

- 331 [25] Hamerton, I. *High Perform. Polym.*, 1996; 8(1): 83-95.
- 332 [26] Venkatesh M, Gouthaman S, Kanemoto S.O., Lakshmi M.S., Hamerton I., *J.Appl. Polym.*
- 333 *Sci.* 2019; 136(28): 47754.
- 334 [27] Ramirez M.L., Walters R., Lyon R.E., Savitski E.P., *Polym. Degrad. Stab.*, 2002; 78(1):73-
- 335 82
- 336 [28] Lyon R.E., Walters R.N., Gandhi S., *Fire Mater.*, 2006; 30(2): 89–106
- 337 [29] Van Krevelen D.W., *Polymer*, 1975; 16(8): 615–620
- 338 [30] Nelson M.I., *Combust. Theor. Model.*, 2001; 5(1): 59-83
- 339 [31] Horrocks A.R., Price D., Tunc M., *J. Appl. Polym. Sci.*, 1989; 37(4): 1051-1061
- 340 [32] Fenimore C.P., In *Flame-Retardant Polymeric Materials*, New York: Plenum, 1975; 1: 371-
- 341 397
- 342 [33] Doyle C.D., *Anal. Chem.*, 1961; 33(1): 77–79
- 343 [34] Pashaei, S., Avval, M.M., Syed, A.A., *Chem. Ind. Chem. Eng. Quart.* 2011; 17(2): 141–151
- 344 [35] Holubka J.W., Devries J.E., Dickie R.A., *Ind. Eng. Chem. Prod. Res. Dev.*, 1984; 23(1): 63-
- 345 70
- 346 [36] Al-Mulla A., Shaban H.I., *Int. J. Polym. Mater.*, 2008; 57(3): 275-287
- 347 [37] Muralidhara K.S., Sreenivasan S., *World Appl. Sci. J.*, 2010; 11(2): 184-189
- 348 [38] Ashok M.A., Achar B.N., *Bull. Mater. Sci.*, 2008; 31(1): 29-35
- 349 [39] Laufer G., Kirkland C., Morgan A.B., Grunlan J.C, *ACS Macro. Lett.*, 2013; 2(5): 361-365